

Controllable generation of two-mode-entangled states in two-resonator circuit QED with a single gap-tunable superconducting qubit

Sheng-Li Ma, Zhen Li, Ai-Ping Fang, Peng-Bo Li, Shao-Yan Gao, and Fu-Li Li*

Department of Applied Physics, School of Science, Xi'an Jiaotong University, Xi'an 710049, People's Republic of China

(Received 19 October 2014; published 29 December 2014)

We study controllable generation of two-mode-entangled states in a circuit QED setup, which consists of two spatially separated superconducting transmission line resonators and a single gap-tunable superconducting qubit. Two sharp coupling sidebands are induced when the artificial atom is suitably driven by a bichromatic microwave field. The two resonators can have squeezing-type interactions with the qubit via the coupling sidebands. If the two resonators are not degenerate, we show that the two resonators can be cooled down into the two-mode squeezed vacuum via dissipation of the qubit. The generation of the two-mode squeezed state is based on a dissipative state-engineering process, which explores the energy relaxation of the qubit as a resource. Moreover, the scheme does not need both the specific preparation of the initial state and the designed special dynamical process of the system. If the resonators are degenerate, we show that entangled coherent states of the resonators can be generated by use of the unitary dynamical evolution process of the system and the state-projection measurement. Moreover, macro entangled coherent states of the resonators with huge photons can in principle be created if the resonators and the qubit have sufficiently long lifetimes. The present scheme has two remarkable features: (1) only a single qubit is used in the generation of the two-mode squeezed state; and (2) the ultrastrong coupling condition and initializing the resonators in coherent states are not required. These make the present scheme more simple and feasible in experimental implementation.

DOI: [10.1103/PhysRevA.90.062342](https://doi.org/10.1103/PhysRevA.90.062342)

PACS number(s): 03.67.Bg, 85.25.Cp, 42.50.Dv

I. INTRODUCTION

The circuit QED, in which Josephson-junction-based artificial atoms interact with a quantized electromagnetic field inside a superconducting resonator, has already proven to be a useful tool for the present-day realization of quantum information protocols [1–3]. These solid-state superconducting circuits have many merits such as flexibility, tunability, and scaling on-chip with nanofabrication techniques [4–7]. In addition, elements in superconducting circuits can be strongly coupled to electromagnetic fields, which makes control, storage, and readout robust [8–12]. Up to now, great progress on this subject has been made for realizing quantum control on a chip. Recent experiments have achieved arbitrary control of a single superconducting resonator [13], and two superconducting qubits have been coupled utilizing an on-chip cavity as a quantum bus [14,15]. Moreover, experimental realization of quantum operational gates and entangled states between two superconducting qubits [16–23] as well as three superconducting qubits [24–27] have also been reported.

However, for large-scale quantum computing, one needs to couple many resonators to build versatile architectures [28]. For this goal, the basic building block is the two-resonator circuit QED setup, in which a superconducting qubit acts as a quantum switch to turn on and off the switchable coupling between the two on-chip resonators [29,30]. Based on this composite system, a lot of theoretical schemes have been proposed to manipulate the spatially separated photon modes and engineer quantum states between physically distant cavities [31–40]. More importantly, deterministic generation of NOON entangled states in two superconducting resonators coupled by a phase qubit has been experimentally demonstrated [41].

Two-mode squeezed states of spatially separated resonators are an important resource for many quantum information processes. In the generation of two-mode squeezed vacuum states of spatially separated resonators by the Jaynes-Cummings-type interaction, as usual, two Bogoliubov modes are involved. The realization of the two-mode squeezed vacuum state means to create a common vacuum for both the Bogoliubov modes. To get the goal, one needs two reservoirs which respectively cool down the two Bogoliubov modes simultaneously into the vacuum, or one needs to employ two qubits to couple the two Bogoliubov modes with each other and engineer the two required reservoirs. In order to make the experimental implementation more simple and accessible with current developed techniques, it is desirable to use only a single reservoir or a single qubit. If only a single qubit is used to engineer the cooling reservoirs, however, one of the nonlocal Bogoliubov modes is decoupled from the qubit [37]. As a result, the steady state of the resonators is not unique, depending on both the initial state and the dynamic evolution process of the system. Thus, for generating the two-mode squeezed state with a single qubit, one has to design a specific state-evolution process starting from a definite initial state, which guarantees the Bogoliubov modes to be in the vacuum in the final state [37]. In a recent publication [42], Woolley and Clerk propose a reservoir engineering strategy for generating two-mode squeezed states of two mechanical oscillators via coupling to a driven cavity mode. In that scheme, two nondegenerate Bogoliubov modes of the mechanical oscillators are coupled with two sidebands of the broadband decay spectrum of the cavity field. As a result, the two Bogoliubov modes are equivalent to be simultaneously coupled with two reservoirs and are cooled to the two-mode squeezed state via the decay of the cavity field.

In this paper, we consider two spatially separated superconducting transmission line resonators that are coupled by

*fli@mail.xjtu.edu.cn

a single two-color-driven superconducting qubit. Two sharp sideband transitions of the qubit can be induced by the driving fields. The two resonators have squeezing-type interaction with the qubit via the sideband transitions. If the two resonators are not degenerate, we show that the two resonator modes can be cooled down into the two-mode squeezed vacuum via dissipation of the qubit. Here, the qubit decay is utilized as a resource to engineer the target state. It has been recognized that the dissipative steady-state production process requires neither the initial state preparation nor the unitary dynamics and has significant advantages in practice [42–45]. On the other hand, only a single qubit is used in the present scheme. Compared with previous schemes such as that in Ref. [46], it may be more simple and feasible in the experimental implementation. If the resonators are degenerate, we show that entangled coherent states of the resonators can be generated by use of the unitary dynamical evolution process of the system and the state-projection measurement. Compared with previous proposals, the present scheme does not need the ultrastrong coupling condition [47] and initializes the resonators in coherent states [48]. Moreover, macro entangled coherent states of the resonators with huge photons can in principle be created if the resonators and the qubit have sufficient long lifetimes. The present work may have interesting applications for implementing distributed quantum computation with a circuit QED system.

The paper is organized as follows. The model describing two spatially separated superconducting transmission line resonators coupled by a single gap-tunable qubit is introduced in Sec. II. The effective Hamiltonian is derived and the generation of two-mode squeezed states of the resonators via dissipation of the qubit is investigated in Sec. III. The generation of entangled coherent states of the resonators is investigated by use of the unitary dynamical evolution process of the system and the state-projection measurement in Sec. IV. The experimental feasibility of the present scheme is discussed in Sec. V. Finally, a summary of the main results is given in Sec. VI.

II. MODEL

As illustrated in Fig. 1, the circuit QED architecture under consideration consists of two on-chip microwave resonators which are coupled to a common gap-tunable superconducting qubit. The qubit is used as a quantum switch to turn on and off the coupling between the resonators. The Hamiltonian of the qubit and the resonators is (let $\hbar = 1$)

$$H_0 = \frac{\delta}{2}\sigma_z + \sum_{j=1}^2 \omega_j a_j^\dagger a_j, \quad (1)$$

where the superconducting qubit is assumed to be operated at the degeneracy point, δ is the static energy gap between the

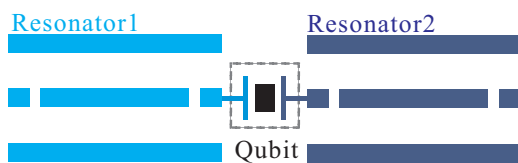


FIG. 1. (Color online) Two superconducting transmission line resonators are connected by a gap-tunable superconducting qubit.

ground state $|g\rangle$ and the excited state $|e\rangle$ of the qubit, $\sigma_z = (|e\rangle\langle e| - |g\rangle\langle g|)$; a_j^\dagger (a_j) is the creation (annihilation) operator for photons in the j th resonator, and ω_j is the corresponding resonator eigenfrequency. The interaction between the qubit and the two resonators takes the form

$$H_I = \sum_{j=1}^2 g_j (\sigma_+ + \sigma_-) (a_j^\dagger + a_j), \quad (2)$$

where g_j is the coupling strength between the qubit and the j th resonator, and $\sigma_+ = |e\rangle\langle g|$, $\sigma_- = |g\rangle\langle e|$.

Commonly, the energy gap between two states of a qubit is fixed. In real applications, however, one needs qubits with a tunable gap. For example, to build a network for quantum computing and information processing, qubits need be coupled with each other or to other subsystems of different transition frequencies. In this way, one needs the energy gap of qubits to be tunable to make resonant couplings between qubits and implement different types of couplings. In the present scheme, we need the energy gap to be tunable to create sidebands of the coupling between the qubit and the resonators and realize the two-mode-squeezing-type interaction. In experiments, various types of gap-tunable superconducting qubits are available such as flux [49], charge [50], and transmon qubits [51]. The *in situ* tunability of the minimum energy gap of a superconducting flux qubit has also been experimentally demonstrated [52]. As usual, a superconducting flux qubit is composed of three Josephson junctions forming a loop, in which two junctions have the same large critical currents but the third junction has the smaller critical current. Note that energy gap of a flux qubit at the degenerate point strongly depends on the critical current of the third junction. For the realization of a gap-tunable flux qubit, the third junction is replaced by two parallel junctions forming a low-inductance dc superconducting quantum interference device (SQUID) loop. Then, the energy gap can be tuned by applying an external magnetic field, penetrating the SQUID loop [52]. When a two-color magnetic field of frequencies ω_{dl} ($l = 1, 2$) is applied to the SQUID loop, we can realize the σ_z -driving

$$H_d(t) = - \sum_{l=1}^2 \xi_l \omega_{dl} \cos(\omega_{dl} t) \sigma_z, \quad (3)$$

where ξ_l ($l = 1, 2$) are the ratios of the driving amplitudes to the driving frequencies. This Hamiltonian presents the periodical modulated energy gap of a flux qubit.

III. GENERATION OF THE TWO-MODE SQUEEZED VACUUM STATE

In this section, we study how to engineer a two-mode squeezed vacuum state of the resonator fields. The key idea of our scheme is to design an appropriate interaction between the qubit and the resonators and bring the system into the desired state by means of the dissipation of the qubit.

If the qubit is coupled to a harmonic oscillator environment in the Markovian approximation, the master equation for the density matrix ρ of the system is given by

$$\frac{d\rho}{dt} = -i [H, \rho] + \Gamma D[\sigma_-] \rho, \quad (4)$$

where $H=H_0+H_I+H_d(t)$, $D[\sigma_-]\rho=(2\sigma_-\rho\sigma_+-\rho\sigma_+\sigma_--\sigma_+\sigma_-\rho)$ is the standard Lindblad operator and Γ represents the energy relaxation rate of the qubit. Here, the decay of the resonators is not taken into account since high- Q transmission line resonators can be achieved in current experiments [62].

In the frame rotated by the unitary transformation $U_1(t)=e^{-iH't}$ with $H'=\frac{\delta}{2}\sigma_z+\sum_{j=1}^2\omega_0a_j^\dagger a_j$ and $\omega_0=\omega_1-\Omega=\omega_2+\Omega$, the total Hamiltonian is

$$H=H_d(t)+\Omega(a_1^\dagger a_1-a_2^\dagger a_2)+\left\{\sum_{j=1}^2g_j e^{i\delta t}\sigma_+(e^{i\omega_0 t}a_j^\dagger+e^{-i\omega_0 t}a_j)+\text{H.c.}\right\}. \quad (5)$$

Then, performing another unitary transformation $U_2(t)=T\exp[-i\int_0^t H_d(t')dt']=e^{i\sum_{l=1}^2\xi_l\sin(\omega_{dl}t)\sigma_z}$, in which T is the time order operator, and keeping the parameters ξ_l to the first order if ξ_l are assumed to be sufficiently small, we have

$$H=\Omega(a_1^\dagger a_1-a_2^\dagger a_2)+\left\{\sum_{j=1}^2g_j\sigma_+e^{i\delta t}(e^{i\omega_0 t}a_j^\dagger+e^{-i\omega_0 t}a_j)\times\left[1-\sum_{l=1}^2\xi_l(e^{i\omega_{dl}t}-e^{-i\omega_{dl}t})\right]+\text{H.c.}\right\}. \quad (6)$$

In order to obtain the desired interaction, we choose the frequencies to satisfy $\omega_{d1}=\delta-\omega_0$ and $\omega_{d2}=\delta+\omega_0$, that is, $\omega_{d1}=\delta-\omega_1+\Omega=\delta-\omega_2-\Omega$, $\omega_{d2}=\delta+\omega_1-\Omega=\delta+\omega_2+\Omega$. In this way, the qubit can be coupled to the resonators by the two sideband transitions, as shown in Fig. 2. If the condition $\{\omega_j,\delta,\omega_{dl}\}\gg g_j,\Omega$ holds, those fast oscillating terms in Eq. (6) can be completely discarded in the rotating wave approximation. Then, we achieve the effective Hamiltonian

$$H_{\text{eff}}=\Omega(a_1^\dagger a_1-a_2^\dagger a_2)+\left\{\sum_{j=1}^2\sigma_+(\Theta_1 a_j+\Theta_2 a_j^\dagger)+\text{H.c.}\right\}, \quad (7)$$

where $g_1=g_2=g$, $\Theta_1=\xi_1 g$, and $\Theta_2=\xi_2 g$ have been set. In the present scheme, a flux qubit is employed and the interaction

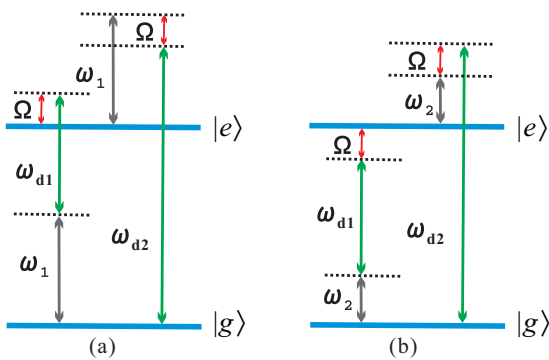


FIG. 2. (Color online) Schematic of sideband transitions of the qubit for generating the two-mode squeezed vacuum state. (a) Sideband coupling between the resonator of frequency ω_1 and the qubit. (b) Sideband coupling between the resonator of frequency ω_2 and the qubit.

between the qubit and the resonators can be realized via the magnetic coupling. As a result, the coupling strength is easily adjusted to satisfy the approximation condition by changing distance of the cavity end to the qubit loop surface.

Note that by performing the unitary transformations $U_1(t)$ and $U_2(t)$, the density operator ρ of the system is changed to $\bar{\rho}=U_2(t)U_1(t)\rho U_1^\dagger(t)U_2^\dagger(t)$, and the relaxation term of Eq. (4) reserves its form except with the replacement of ρ by $\bar{\rho}$. Then, we perform the two-mode squeezing transformation $S(\zeta)=e^{\zeta a_1 a_2 - \zeta^* a_1^\dagger a_2^\dagger}$ to the master equation for the density operator $\bar{\rho}$ with the effective Hamiltonian (7), where the squeezing degree $\zeta=\tanh^{-1}(\xi_2/\xi_1)$. In the squeezing representation, we have

$$\frac{d\tilde{\rho}}{dt}=-i[\tilde{H}_{\text{eff}},\tilde{\rho}]+\Gamma D[\sigma_-]\tilde{\rho}, \quad (8)$$

with

$$\tilde{H}_{\text{eff}}=\Omega(a_1^\dagger a_1-a_2^\dagger a_2)+\sum_{j=1}^2\sqrt{\Theta_1^2-\Theta_2^2}(\sigma_+ a_j+\sigma_- a_j^\dagger). \quad (9)$$

It now becomes clear that if the vacuum state $|0,0\rangle_{1,2}=|0\rangle_1|0\rangle_2$ of the resonator modes a_1 and a_2 is the unique steady state of Eq. (8) in the squeezing representation, going back to the original representation, the steady state is the two-mode squeezed vacuum state $S(\zeta)|0,0\rangle_{1,2}=e^{\zeta a_1 a_2 - \zeta^* a_1^\dagger a_2^\dagger}|0,0\rangle_{1,2}$. In the following, we show that $|0,0\rangle_{1,2}$ is indeed the unique steady state of Eq. (8).

For this goal, we define two normal boson modes $A_1=(a_1+a_2)/\sqrt{2}$ and $A_2=(a_1-a_2)/\sqrt{2}$. In terms of the operators A_1 and A_2 , Eq. (8) can be rewritten in the form

$$\frac{d\tilde{\rho}}{dt}=-i[\tilde{H}_{\text{eff}},\tilde{\rho}]+\Gamma D[\sigma_-]\tilde{\rho}, \quad (10)$$

with

$$\tilde{H}_{\text{eff}}=\Omega(A_1 A_2^\dagger+A_1^\dagger A_2)+\sqrt{2(\Theta_1^2-\Theta_2^2)}(\sigma_+ A_1+\sigma_- A_1^\dagger). \quad (11)$$

Note that the second term $\sqrt{2(\Theta_1^2-\Theta_2^2)}(\sigma_+ A_1+\sigma_- A_1^\dagger)$ in Eq. (11) describes a Jaynes-Cummings-type interaction between the qubit and the mode A_1 . Hence, the mode A_1 can directly be cooled down to the vacuum by the Jaynes-Cummings interaction and the energy relaxation described by $\Gamma D[\sigma_-]\tilde{\rho}$. On the other hand, the quanta in mode A_2 will be continuously swapped into mode A_1 , and then absorbed by the qubit due to the interaction between A_1 and A_2 described by the first term $\Omega(A_1 A_2^\dagger+A_1^\dagger A_2)$ in Eq. (11). Thus, both the modes A_1 and A_2 will be cooled to the vacuum at the steady state via the dissipative process of the qubit. Reversing the squeezing transformation $S(\zeta)$ to the resulting vacuum state, we obtain the unique steady state $|\Psi_S\rangle$ of the system

$$|\Psi_S\rangle=e^{\zeta a_1 a_2 - \zeta^* a_1^\dagger a_2^\dagger}|0,0\rangle_{1,2}\otimes|g\rangle. \quad (12)$$

As is seen in the above discussion, the two superconducting resonators are steered into the two-mode squeezed state by means of the dissipative steady-state production process of the qubit. It is noticed that the second term of Eq. (11) shows

the mode A_2 decoupled from the qubit. If the first term of Eq. (11) was absent, the decay of the qubit would have no any action to the mode A_2 and the steady state of the mode A_2 would be uncertain. That is why one has to design the adiabatical process to get the desired state in steady state in the previous investigation [37]. In the present scheme, the mode A_2 is coupled to the mode A_1 by the first term of Eq. (11) and is cooled down to its vacuum with the assistance of the the mode A_1 by the dissipation of the qubit. In the present generation process, therefore, one need not precisely control the evolution time and initialize states of both the resonators and the qubit. Thus, our scheme turns a detrimental source of noise into a resource and has significant advantages in practice. Furthermore, the present scheme provides a tunable two-mode squeezed vacuum resource; that is, we can adjust the degree of squeezing on demand by changing the ratio of the external parameters ξ_2 to ξ_1 . The engineered two-mode squeezed states are of crucial importance for implementing various quantum information protocols, such as quantum key distribution, entanglement swapping, error correction, and full-fledged quantum computing [54]. In experiments, we can also detect the microwave field entanglement between the two resonators by a frequency-dependent variant of the cross-correlation methods [55,56].

To quantify the squeezing with experimentally attainable parameters, we numerically solve the master Eq. (4) including the decay of the cavity modes. In the calculation, we choose $Q = Q_1 = Q_2$, and the cavity decay rate $\kappa_j = \omega_j/Q$. As usual, we introduce the two quadrature components $u = X_1 + X_2, v = P_1 - P_2$ with $X_\lambda = (a_\lambda + a_\lambda^\dagger)/\sqrt{2}, P_\lambda = -i(a_\lambda - a_\lambda^\dagger)/\sqrt{2}$ ($\lambda = 1, 2$), and build the squeezing or entanglement criterion. It has been shown that the variance $V = \langle (\Delta u)^2 + (\Delta v)^2 \rangle$ is always smaller than 2 for an entangled two-mode state [57]. For the numerical calculation, the system is initially prepared in the ground state $|0, 0\rangle_{1,2} \otimes |g\rangle$. In Fig. 3, the steady-state variances versus the ratio ξ_2/ξ_1 are plotted, where the solid, dash-dotted, dashed, and dotted lines

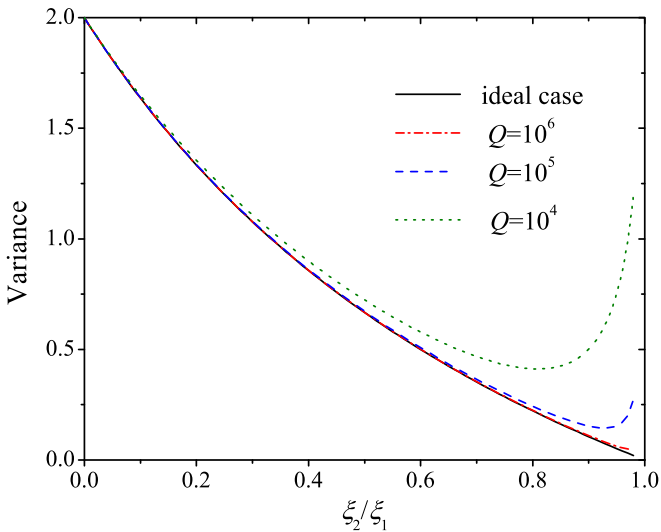


FIG. 3. (Color online) Variance vs the ratio ξ_2/ξ_1 . The relevant parameters are chosen to be $\delta/2\pi = 10$, $\omega_1/2\pi = 6.04$, $\omega_2/2\pi = 6$, $g/2\pi = 0.1$, $\Gamma/2\pi = 0.02$, $\Omega/2\pi = 0.02$ GHz, and $\xi_1 = 0.2$.

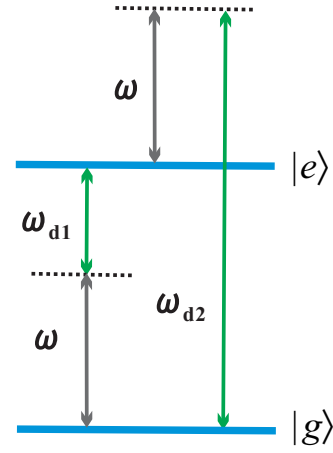


FIG. 4. (Color online) Schematic of sideband transitions of the qubit for preparing entangled coherent state.

respectively represent the situations of the ideal squeezed vacuum ($V = 2e^{-2\xi}$), and $Q = 10^6, 10^5, 10^4$. With the most achievable value $Q = 10^6$ in current experiments, as shown in Fig. 3, the variance (dash-dotted line) versus the ratio ξ_2/ξ_1 has almost no divergence from the ideal case (solid line). Thus, our scheme provides a tunable two-mode squeezed vacuum source and can be implemented by the existing experimental technologies.

IV. GENERATION OF THE TWO-MODE-ENTANGLED COHERENT STATE

In this section, we discuss how to generate an entangled coherent state in the two spatially separated resonators. Unlike in the previous section, the generation is based on the coherent control to the unitary evolution of the system. Thus, the superconducting qubit needs to possess a long coherence time. In addition, we assume that the two superconducting resonators have same eigenfrequencies $\omega = \omega_1 = \omega_2$.

After the rotation transformation $U_1(t) = e^{-iH_0t}$, the Hamiltonian of the system is changed to

$$H = H_d(t) + \left\{ \sum_{j=1}^2 g_j e^{i\delta t} \sigma_+ (e^{i\omega t} a_j^\dagger + e^{-i\omega t} a_j) + \text{H.c.} \right\}. \quad (13)$$

Then, performing the unitary transformation $U_2(t) = T \exp[-i \int_0^t H_d(t') dt'] = e^{i \sum_{l=1}^2 \xi_l \sin(\omega_{dl} t) \sigma_z}$, and keeping the parameter ξ_l only to the first order, we have

$$H = \sum_{j=1}^2 g_j \sigma_+ e^{i\delta t} (e^{i\omega t} a_j^\dagger + e^{-i\omega t} a_j) \times \left[1 - \sum_{l=1}^2 \xi_l (e^{i\omega_{dl} t} - e^{-i\omega_{dl} t}) \right] + \text{H.c.} \quad (14)$$

To get the desired qubit-resonator coupling, we choose $\omega_{d1} = \delta - \omega$ and $\omega_{d2} = \delta + \omega$, which correspond to the qubit subjected to the red sideband and blue sideband excitations [58], as shown in Fig. 4. If the condition $\{\omega, \delta, \omega_{dl}\} \gg g_j$ holds, those fast oscillating terms in Eq. (14) can be discarded in

the rotating-wave approximation. As a result, we achieve the effective Hamiltonian

$$H_{\text{eff}} = \sum_{j=1}^2 \Theta_j (\sigma_+ + \sigma_-) (a_j + a_j^\dagger), \quad (15)$$

where we have set $\xi = \xi_1 = \xi_2$, and $\Theta_j = \xi g_j$.

The dynamics of the system is governed by the unitary evolution operator $e^{-iH_{\text{eff}}t}$. Assume that the system is initially in the ground state $|\psi(t=0)\rangle = |g\rangle \otimes |0,0\rangle_{1,2} = |g\rangle \otimes |0\rangle_1 |0\rangle_2$, where the resonators are decoupled from the qubit before we turn on the two-color modulation field. After the σ_z driving to the qubit is turned on, the system will evolve into the state at time t

$$|\psi(t)\rangle = e^{-iH_{\text{eff}}t} |\psi(t=0)\rangle. \quad (16)$$

In the representation spanned by the new basis vectors $|\pm\rangle = (|e\rangle \pm |g\rangle)/\sqrt{2}$, we rewrite the initial state $|\psi(t=0)\rangle = (|+\rangle - |-\rangle)/\sqrt{2} \otimes |0\rangle_1 |0\rangle_2$, as well as the unitary time-evolution operator $e^{-iH_{\text{eff}}t} = \otimes_{j=1}^2 D(\alpha_j) |+\rangle\langle +| + D(-\alpha_j) |-\rangle\langle -|$, in which $D(\alpha_j)$ is the unitary displacement operator $D(\alpha_j) = e^{\alpha_j a_j^\dagger - \alpha_j^* a_j}$ with the coherent amplitude $\alpha_j = -i\Theta_j t$. Correspondingly, the state at time t can be rewritten in the form

$$|\psi(t)\rangle = \frac{\sqrt{2}}{2} (|+\rangle |\alpha_1\rangle |\alpha_2\rangle - |-\rangle |-\alpha_1\rangle |-\alpha_2\rangle), \quad (17)$$

where $|\alpha_j\rangle$ is the coherent state $|\alpha_j\rangle = D(\alpha_j)|0\rangle_j$. This state represents an elaborate tripartite entangled state involving one qubit and two resonator modes. At time t , we turn off the external driving to the qubit, and then the interaction between the qubit and the resonators is shut down. After the moment t , the system will have stayed in the tripartite entangled state if no any dissipation processes are involved.

In the representation spanned by the original basis vectors $|g\rangle$ and $|e\rangle$, Eq. (17) takes the form

$$|\psi(t)\rangle = \frac{1}{2} [|g\rangle (|\alpha_1\rangle |\alpha_2\rangle + |-\alpha_1\rangle |-\alpha_2\rangle) + |e\rangle (|\alpha_1\rangle |\alpha_2\rangle - |-\alpha_1\rangle |-\alpha_2\rangle)]. \quad (18)$$

Now let us consider a state-projection measurement to the qubit. When the measured result shows the qubit to be in the state $|g\rangle$ ($|e\rangle$), the resonators collapse into the entangled coherent state $|\psi_+\rangle$ ($|\psi_-\rangle$), which are given by

$$|\psi_\pm\rangle = \frac{|\alpha_1\rangle |\alpha_2\rangle \pm |-\alpha_1\rangle |-\alpha_2\rangle}{\sqrt{2 \pm 2 \exp(-2|\alpha_1|^2 - 2|\alpha_2|^2)}}. \quad (19)$$

These entangled coherent states not only have potential applications in the fundamental quantum theory but also are a valuable resource in the field of quantum information processing [59,60].

To quantify entanglement of the resulting entangled coherent states, we explore the concurrence of the states [61]. The concurrence C_\pm of the states $|\psi_\pm\rangle$ are given by

$$C_\pm = \frac{\sqrt{[1 - \exp(-4|\alpha_1|^2)][1 - \exp(-4|\alpha_2|^2)]}}{1 \pm \exp(-2|\alpha_1|^2 - 2|\alpha_2|^2)}. \quad (20)$$

The concurrences C_+ and C_- versus the parameters $|\alpha_1|$ and $|\alpha_2|$ are shown in Figs. 5(a) and 5(b), respectively. It is observed that in the area of $|\alpha_1| \geq 1$ and $|\alpha_2| \geq 1$, the

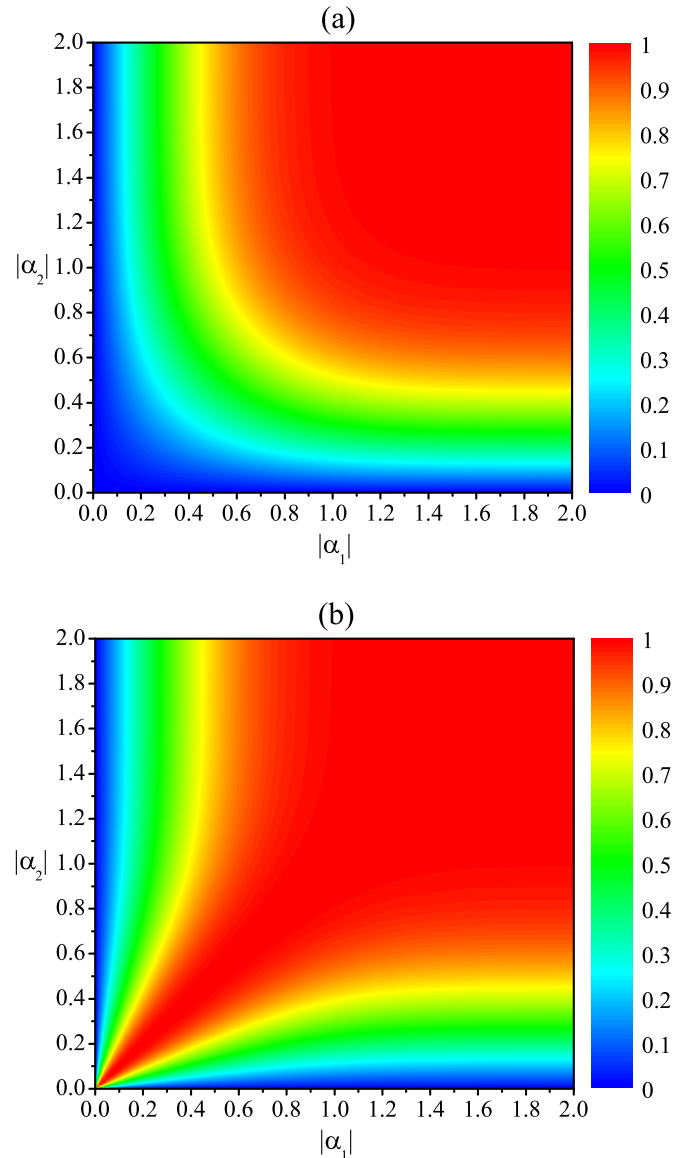


FIG. 5. (Color online) (a) Concurrence C_+ vs the parameters $|\alpha_1|$ and $|\alpha_2|$ for the even entangled coherent state $|\psi_+\rangle$. (b) Concurrence C_- vs the parameters $|\alpha_1|$ and $|\alpha_2|$ for the odd entangled coherent state $|\psi_-\rangle$.

concurrences C_\pm reach 1. It means that in the region the states $|\psi_\pm\rangle$ are maximally entangled states. Here, we emphasize that the realization of those maximally entangled coherent states is very difficult in the previous scheme [47] with the currently available technique. Note that the parameter $|\alpha_j|$ is determined by the ratio g_j/ω_j ($j = 1,2$) in Ref. [47]. To achieve the maximally entangled coherent states, therefore, the coupling strength g_j is required to approach the eigenfrequency ω_j . It means that the scheme has to work in the ultrastrong coupling regime. Even if the ultrastrong coupling regime $g_j/\omega_j \sim 12\%$ for a flux qubit and a transmission line resonator has been realized in experiment [62], it is still a huge challenge to reach the regime $g_j/\omega_j \sim 1$. However, in our scheme, the condition $|\alpha_j| = |\Theta_j t| \geq 1$ ($j = 1,2$) can be easily realized without the ultrastrong coupling if the resonators and the qubit have a long

coherent time. In Fig. 5(b), we observe that the concurrence C_- can also get 1 and the maximally entangled coherent state can be realized even if both $|\alpha_1|$ and $|\alpha_2|$ are very small. It means that the present scheme need not have both the ultrastrong coupling condition and long coherent evolution time for generating entangled coherent states with a small mean photon number. Of course, one needs to have a sufficiently large average photon number $|\alpha|^2$ for making the entangled coherent states be truly macroscopic states. In this sense, it requires that the qubit and the resonators should have sufficiently long lifetimes. In addition, compared with the previous scheme [48], our scheme does not need initially prepared resonators in coherent states and needs only dynamical modulation of the energy gap of the qubit. Therefore, our scheme is more feasible in experimental implementation.

V. EXPERIMENTAL FEASIBILITY

The rapid development in superconducting quantum circuits holds great promise for the experimental feasibility of our schemes. In principle, our scheme can be implemented with all kinds of superconducting resonators interconnected by a gap-tunable superconducting qubit, such as flux [49], charge [50], or transmon qubits [51], which have the ability to induce sidebands in the qubit-resonator coupling. In the practical situations, the transmission line resonator with a quality factor $\sim 10^6$ is the most relevant value in experiment, and higher Q factor approaching 10^8 has been achieved [53]. In addition, the superconducting qubit coupled to a high-quality microwave resonator can easily reach the strong coupling g of hundreds of MHz [13,14]. For the generation of two-mode squeezed vacuum state, we need a “bad” qubit with large decay rate to implement the dissipative quantum dynamical process. This can be engineered by coupling the qubit with an auxiliary bath, such as an open transmission line that provides a relaxation channel [58]. For the generation of entangled coherent state, we need the superconducting qubit with a long coherence time. The coherence time of current well-designed qubits is $100 \mu\text{s}$ and is growing steadily [53]. It is sufficient to implement the our proposed protocol. On the other hand, the measurement of the qubit may cause decoherence and decrease the fidelity of the final state. However, a recently developed multiplexed measurement system allows fast measurement without increasing environmental damping of the qubits; that is, the qubit can be measured to 99.8% accuracy with a high speed of 140 ns [63]. Most importantly, the deterministic

generation of entangled photon states in two spatially separated microwave resonators connected by a superconducting phase qubit has been experimentally demonstrated [41]. Thus, we believe that the present scheme is achievable based on the existing experimental technologies.

VI. CONCLUSION

We have proposed a scheme for generating two-mode microwave photon entangled states in two spatially separated superconducting resonators which are coupled by a single gap-tunable superconductor. Two sharp sideband transitions of multiphoton resonance of the qubit can be induced by a bichromatic microwave driving field. In this way, two electromagnetic modes of the resonators are coupled to the qubit via the two sideband transitions. If the two resonators are not degenerate, we show that two modes of the resonators can be cooled down into the two-mode squeezed vacuum via dissipation of the qubit. The generation of the two-mode squeezed state is based on a dissipative state-engineering process, which explores the energy relaxation of the qubit as a resource. Moreover, this scheme does not need both the specific preparation of the initial state and the designed special dynamical process of the system. Since only is a single qubit used, the present scheme may be more simple and feasible in experimental implementation. If the resonators are degenerate, we show that entangled coherent states of the resonators can be generated by use of the unitary dynamical evolution process of the system and the state-projection measurement. It is a remarkable feature that the present scheme does not need the ultrastrong coupling condition and initialization of the resonators in coherent states. Moreover, macro entangled coherent states of the resonators with huge photons can in principle be created if the resonators and the qubit have sufficiently long lifetimes. Note that the recent experiment demonstrates the excellent quantum control over photon Fock states in three resonators interconnected by two qubits [64]. This progress makes us believe it is possible to extend the present scheme to more complicated architectures.

ACKNOWLEDGMENTS

This work was supported by the National Natural Science Foundation of China (Grants No. 11374239 and No. 11104215), and the Research Fund for the Doctoral Program of Higher Education of China (Grant No. 20110201120035).

-
- [1] J. Clarke and F. K. Wilhelm, *Nature (London)* **453**, 1031 (2008).
 - [2] J. Q. You and F. Nori, *Phys. Today* **58**, 42 (2005).
 - [3] Y. Makhlin, G. Schon, and A. Shnirman, *Rev. Mod. Phys.* **73**, 357 (2001).
 - [4] J. E. Mooij, T. P. Orlando, L. Levitov, L. Tian, C. H. van der Wal, and S. Lloyd, *Science* **285**, 1036 (1999).
 - [5] Y. Yu, S. Han, X. Chu, S. I. Chu, and Z. Wang, *Science* **296**, 889 (2002).
 - [6] G. Wendin and V. S. Shumeiko, *Low Temp. Phys.* **33**, 724 (2007).
 - [7] A. A. Houck, H. E. Tüeci, and J. Koch, *Nat. Phys.* **8**, 292 (2012).
 - [8] A. Lupaşcu, C. J. M. Verwijs, R. N. Schouten, C. J. P. M. Harmans, and J. E. Mooij, *Phys. Rev. Lett.* **93**, 177006 (2004).
 - [9] A. Blais, R.-S. Huang, A. Wallraff, S. M. Girvin, and R. J. Schoelkopf, *Phys. Rev. A* **69**, 062320 (2004).
 - [10] A. Wallraff *et al.*, *Nature (London)* **431**, 162 (2004).
 - [11] I. Chiorescu, P. Bertet, K. Semba, Y. Nakamura, C. J. P. M. Harmans, and J. E. Mooij, *Nature (London)* **431**, 159 (2004).
 - [12] Y. Nakamura, Y. A. Pashkin, and J. S. Tsai, *Nature (London)* **398**, 786 (1999).

- [13] M. Hofheinz *et al.*, *Nature (London)* **459**, 546 (2009).
- [14] M. Sillanpää, J. I. Park, and R. W. Simmonds, *Nature (London)* **449**, 438 (2007).
- [15] J. Majer *et al.*, *Nature (London)* **449**, 443 (2007).
- [16] L. DiCarlo *et al.*, *Nature (London)* **460**, 240 (2009).
- [17] M. Ansmann *et al.*, *Nature (London)* **461**, 504 (2009).
- [18] T. Yamamoto, Y. A. Pashkin, O. Astafiev, Y. Nakamura, and J. S. Tsai, *Nature (London)* **425**, 941 (2003).
- [19] A. J. Berkley *et al.*, *Science* **300**, 1548 (2003).
- [20] T. Hime, P. A. Reichardt, B. L. T. Plourde, T. L. Robertson, C. E. Wu, A. V. Ustinov, and John Clarke, *Science* **314**, 1427 (2006).
- [21] S. H. W. van der Ploeg, A. Izmailkov, A. Maassen van den Brink, U. Hübner, M. Grajcar, E. Il'ichev, H.-G. Meyer, and A. M. Zagoskin, *Phys. Rev. Lett.* **98**, 057004 (2007).
- [22] D. Ristè *et al.*, *Nature (London)* **502**, 350 (2013).
- [23] M. Steffen *et al.*, *Science* **313**, 1423 (2006).
- [24] L. DiCarlo, M. D. Reed, L. Sun, B. R. Johnson, J. M. Chow, J. M. Gambetta, L. Frunzio, S. M. Girvin, M. H. Devoret, and R. J. Schoelkopf, *Nature (London)* **467**, 574 (2010).
- [25] M. Neeley *et al.*, *Nature (London)* **467**, 570 (2010).
- [26] A. Fedorov, L. Steffen, M. Baur, M. P. da Silva, and A. Wallraff, *Nature (London)* **481**, 170 (2012).
- [27] L. F. Wei, Y. X. Liu, and F. Nori, *Phys. Rev. Lett.* **96**, 246803 (2006).
- [28] C. David *et al.*, [arXiv:1402.7036](https://arxiv.org/abs/1402.7036).
- [29] M. Mariani, F. Deppe, A. Marx, R. Gross, F. K. Wilhelm, and E. Solano, *Phys. Rev. B* **78**, 104508 (2008).
- [30] G. M. Reuther *et al.*, *Phys. Rev. B* **81**, 144510 (2010).
- [31] F. Xue, Y. X. Liu, C. P. Sun, and F. Nori, *Phys. Rev. B* **76**, 064305 (2007).
- [32] F. L. Semião, K. Furuya, and G. J. Milburn, *Phys. Rev. A* **79**, 063811 (2009).
- [33] F. W. Strauch, K. Jacobs, and R. W. Simmonds, *Phys. Rev. Lett.* **105**, 050501 (2010).
- [34] Y. Hu and L. Tian, *Phys. Rev. Lett.* **106**, 257002 (2011).
- [35] Z. H. Peng, Y. X. Liu, Y. Nakamura, and J. S. Tsai, *Phys. Rev. B* **85**, 024537 (2012).
- [36] S. T. Merkel and F. K. Wilhelm, *New J. Phys.* **12**, 093036 (2010).
- [37] P. B. Li, S. Y. Gao, and F. L. Li, *Phys. Rev. A* **85**, 014303 (2012).
- [38] S. L. Ma, Z. Li, P. B. Li, and F. L. Li, *Phys. Rev. A* **90**, 043810 (2014).
- [39] C. P. Sun, L. F. Wei, Y. X. Liu, and F. Nori, *Phys. Rev. A* **73**, 022318 (2006).
- [40] W. L. Yang, Z. Q. Yin, Q. Chen, C. Y. Chen, and M. Feng, *Phys. Rev. A* **85**, 022324 (2012).
- [41] H. Wang *et al.*, *Phys. Rev. Lett.* **106**, 060401 (2011).
- [42] M. J. Woolley and A. A. Clerk, *Phys. Rev. A* **89**, 063805 (2014).
- [43] Y. Lin, J. P. Gaebler, F. Reiter, T. R. Tan, R. Bowler, A. S. Sørensen, D. Leibfried, and D. J. Wineland, *Nature (London)* **504**, 415 (2013).
- [44] S. L. Ma, P. B. Li, A. P. Fang, S. Y. Gao, and F. L. Li, *Phys. Rev. A* **88**, 013837 (2013).
- [45] H. Krauter, C. A. Muschik, K. Jensen, W. Wasilewski, J. M. Petersen, J. I. Cirac, and E. S. Polzik, *Phys. Rev. Lett.* **107**, 080503 (2011).
- [46] P. B. Li, S. Y. Gao, and F. L. Li, *Phys. Rev. A* **86**, 012318 (2012).
- [47] M. Y. Chen, M. W. Y. Tu, and W. M. Zhang, *Phys. Rev. B* **80**, 214538 (2009).
- [48] C. P. Yang, Q. P. Su, S. B. Zheng, and S. Y. Han, *Phys. Rev. A* **87**, 022320 (2013).
- [49] Y. X. Liu, L. F. Wei, J. R. Johansson, J. S. Tsai, and F. Nori, *Phys. Rev. B* **76**, 144518 (2007).
- [50] A. Wallraff, D. I. Schuster, A. Blais, J. M. Gambetta, J. Schreier, L. Frunzio, M. H. Devoret, S. M. Girvin, and R. J. Schoelkopf, *Phys. Rev. Lett.* **99**, 050501 (2007).
- [51] P. J. Leek, S. Filipp, P. Maurer, M. Baur, R. Bianchetti, J. M. Fink, M. Göpl, L. Steffen, and A. Wallraff, *Phys. Rev. B* **79**, 180511(R) (2009).
- [52] F. G. Paauw, A. Fedorov, C. J. P. M. Harmans, and J. E. Mooij, *Phys. Rev. Lett.* **102**, 090501 (2009).
- [53] Z.-L. Xiang, S. Ashhab, J. Q. You, and F. Nori, *Rev. Mod. Phys.* **85**, 623 (2013).
- [54] S. L. Braunstein and P. van Loock, *Rev. Mod. Phys.* **77**, 513 (2005).
- [55] D. Bozyigit *et al.*, *Nat. Phys.* **7**, 154 (2010).
- [56] M. Mariani, E. P. Menzel, F. Deppe, M. A. Araque Caballero, A. Baust, T. Niemczyk, E. Hoffmann, E. Solano, A. Marx, and R. Gross, *Phys. Rev. Lett.* **105**, 133601 (2010).
- [57] L. M. Duan, G. Giedke, J. I. Cirac, and P. Zoller, *Phys. Rev. Lett.* **84**, 2722 (2000).
- [58] D. Porras and J. J. Garcia-Ripoll, *Phys. Rev. Lett.* **108**, 043602 (2012).
- [59] W. M. Zhang, D. H. Feng, and R. Gilmore, *Rev. Mod. Phys.* **62**, 867 (1990).
- [60] E. Solano, G. S. Agarwal, and H. Walther, *Phys. Rev. Lett.* **90**, 027903 (2003).
- [61] X. Wang, *J. Phys. A* **35**, 165 (2002).
- [62] T. Niemczyk *et al.*, *Nat. Phys.* **6**, 772 (2010).
- [63] E. Jeffrey, D. Sank, J. Y. Mutus, T. C. White, J. Kelly, R. Barends, Y. Chen, Z. Chen, B. Chiaro, A. Dunsworth, A. Megrant, P. J. J. O'Malley, C. Neill, P. Roushan, A. Vainsencher, J. Wenner, A. N. Cleland, and J. M. Martinis, *Phys. Rev. Lett.* **112**, 190504 (2014).
- [64] M. Mariani *et al.*, *Nat. Phys.* **7**, 287 (2011).